Journal of New Materials for Electrochemical Systems 16, 019-023 (2013)

Improved Commercialized Lithium Titanate Performance in Lithium-ion Batteries by Annealing

Xinxi Li*, Guoqing Zhang, Zhongqiong Xiong, Junqiao Xiong and Yongping Qiu

School of Materials and Energy, Guangdong University of Technology, Guangzhou 510006, PR China

Received: July 28, 2012, Accepted: August 21, 2012, Available online: October 16, 2012

Abstract: *The high rate capability of commercial lithium titanate ($Li_4Ti_5O_{12}$; LTO) is improved by annealing. The commercial LTO particles are calcined at a 650 °C for 4 h. XRD, SEM, BET, PSD and electrochemical tests reveal that annealing the sample results in smaller particle sizes, more uniform particle size distribution, and excellent electrochemical performance. In assembling half of the battery at 1C, 3C, and 5C charge–discharge rates, the discharge capacity of sample A (no carbon) reached 170.7, 164.5, 151.8 $mAhg^{-1}$, respectively, for the first time. The capacity retention rates were 94.6%, 87.6%, and 87.6%, respectively. The discharge capacity of sample B (containing carbon) reached 173.6, 162.7, and 153.5 $mAhg^{-1}$, respectively, for the first time. The capacity retention rates are 94.1%, 90.9%, and 91.8%, respectively. The cycling stability shows almost no improvement, but the reversible capacity is enhanced. A comparison of the electrochemical performances of samples A and B show that the annealing process can play a very important role in carbon-containing samples. The main reason is that carbon itself has good conductivity, whereas carbon coatings also inhibit the grain growth of LTO; smaller grain sizes can shorten the diffusion path of Li^+ and promote the reversible capacities of a material.*

Keywords: annealing; $Li_4Ti_5O_{12}$; lithium ion battery; rate performance

1. INTRODUCTION

Lithium (Li)-ion rechargeable batteries are widely used in portable electronic devices, including laptop computers, mobile phones, and camcorders. These batteries are also very promising power sources for large applications, such as hybrid electric vehicles and electric vehicles[1-3].

Despite the evident advantages of Li-ion batteries over nickel-cadmium and lead-acid cells, i.e., higher energy density and longer cycling life, there are still some safety concerns with the carbon anode[4].

In recent years, graphite as an anode material has attracted much attention due to its peculiar and fascinating properties superior over its bulk counterparts and potential applications in various fields. There is increasing interest in Li titanate as material for Li-ion batteries with excellent performance.

Spinel $Li_4Ti_5O_{12}$ (LTO) has been demonstrated as a good anode candidate for solid–state Li-ion batteries [5–8]. It has good Li ion intercalation and de-intercalation reversibility, and no structural change during the charge–discharge cycling. It also generates $Li_7Ti_5O_{12}$ unit cell parameters with very small changes, only increasing from 0.836 nm to 0.837 nm, thus termed zero-strain electrodes [9].

LTO has a high Coulombic efficiency (near 100%), and its Li–ion diffusion coefficient is higher than an ordinary carbon negative electrode by an order of magnitude ($2 \times 10^{-8} cm^2/s$). LTO also has very excellent characteristics, such as being clean and green, extensive range of material sources, and so on [14]. Therefore, LTO as an anode material for Li-ion batteries can be effectively improve the battery performance, rapid charge and discharge cycle performance, and security capability. Recently, its use as a dynamic type high-power Li–ion battery anode material has become a popular topic.

In most studies, LTO powders have been successfully synthesized by solid–state reaction [15, 16], electrostatic spray deposition [17], ball-milling [18, 19], sol–gel method [20], spray-drying/pyrolysis [21, 22], and so on. As for the sol–gel synthesis of LTO, high-temperature calcination at 800 °C or higher is necessary to prepare a pure spinel phase, which results in undesirable particle growth.

Despite the high temperature of the solid–state reaction synthesis of titanium Li ion, its size tends toward the micron or sub-

*To whom correspondence should be addressed: Email: gdutlxx@163.com

micron level, and the particle size distribution is non-uniform, mixed, and limited [23]. Using this method for the synthesis of LTO crystal can result in defects and affect the electrochemical properties [24]. However, this process is very simple, low cost, and suitable for mass production.

At present, commercial LTO is produced via solid–state reaction synthesis under high temperatures. However, its performance as a battery material can be affected by each step of the process it undergoes, from the commercialization of its products to its application in batteries. Studies have shown that the electrochemical performance of Li titanate powders decay under the dew point of –50 °C, or when stored in a dry warehouse for a long time [25].

The next generation of battery materials is expected to maintain the electrochemical properties of the commercial product even during storage, thus improving its reversible capacity and cycling performance. Studies indicate that the annealing process can improve the electrochemical properties of Li titanate materials [26]. Setiawati et al. [25] have found that the electrochemical performance of Li titanium oxide with a ramsdellite structure is significantly improved by annealing in a chamber furnace. Annealing treatment is simple, safe, and environmentally friendly. These advantages are of great value to a commercial material.

The present study attempts to improve the structure of commercialized LTO by annealing. The results show that the process can not only make the grain distribution more uniform, but also significantly improve the electrochemical properties.

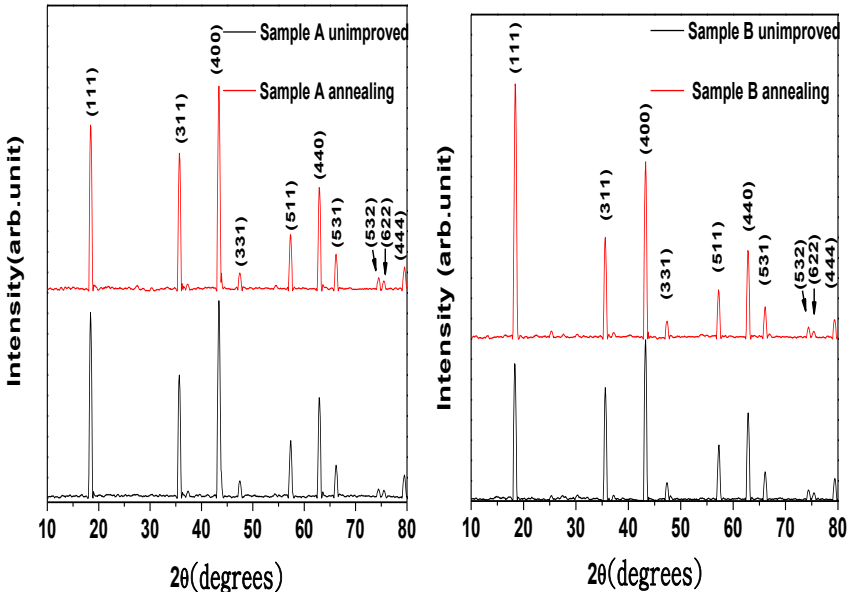

Figure 1. X-ray diffraction patterns of $Li_4Ti_5O_{12}$: (a) sample A and (b) sample B.

2. EXPERIMENTAL

2.1. Annealing of the commercial LTO samples

The commercial LTO samples were prepared using the company of ShenZhenTianJiao (no carbon, sample A) and company of HuNanShanShan (containing carbon, sample B) Li titanate. The experiment was performed by low-temperature annealing. The samples were oven dried for 12 h before annealing, and placed in a mortar. The powder was then heated evenly. The resulting product, Sample B, was calcined under flowing nitrogen, ensuring that it did not interfere with the chemical inertia of carbon. Sample A can be calcined in the presence of oxygen because it did not contain carbon. It was calcined at 650 °C for 4 h.

2.2. Physical characterization

Powder X-ray diffraction (XRD) patterns were collected on a Rigaku D/MAX-rA diffractometer with CuKα radiation (λ = 1.5418 Å) operating at 40 kV and 100 mA. A scanning electron microscopy (SEM) system (Hitachi S–450, Japan) was used to observe the grain morphology and particle size. Particle size distribution (PSD) was analyzed using a Nanotrac 150 particle size analyzer. Brunauer–Emmett–Teller (BET) surface area was measured with Micromerities Gemini V instruments.

2.3. Electrochemical measurements

The electrochemical properties of the LTO electrodes were determined from Li/1 M LiPF6 in ethylene carbonate and diethyl carbonate (1:1, w/w)/LTO cells using a LAND Battery Program-control Test System. The LTO electrodes were fabricated by mixing 85:10:5 (w/w) of active material, a carbon (acetylene black) electronic conductor, and a polyvinylidene fluoride binder, using N-methyl-2-pyrrolidine as solvent. After drying the obtained slurry overnight under a vacuum at 100 °C, the mixture was pressed onto an aluminum sheet. Li was used as the counter electrode. The cells were assembled in a glove box. Charge–discharge cycle tests were performed at a constant current density of 0.5 mA/cm^2 over a potential range of 1 V to 3.0 V.

3. RESULTS AND DISCUSSION

3.1. XRD analysis

The XRD patterns of LTO and LTO-650 °C composite materials are presented in Fig. 1 which shows no obvious miscellaneous phase in the XRD patterns of LTO. All diffraction peaks can be indexed based on a face-centered cubic spinel structure with an Fd3m space group. The LTO composite material shows that the peaks at 2θ = 18.3°, 35.6°, 43.2°, 57.2°, and 62.9° are indexed as the (111), (311), (400), (432), (333), and(440) reflections of LTO, respectively. The location and relative strength of its characteristic peaks correspond to the LTO standard XRD spectrum. After annealing, the peak becomes narrow and the diffraction intensity increases. This phenomenon shows that annealing is a very effective method for obtaining highly crystalline LTO.

3.2. SEM analysis

Fig. 2 shows the scanning electron micrograph of samples A and B. The morphology of the LTO appears to be regular cubic spinel with good dispersivity, and the particle sizes are homogeneous with

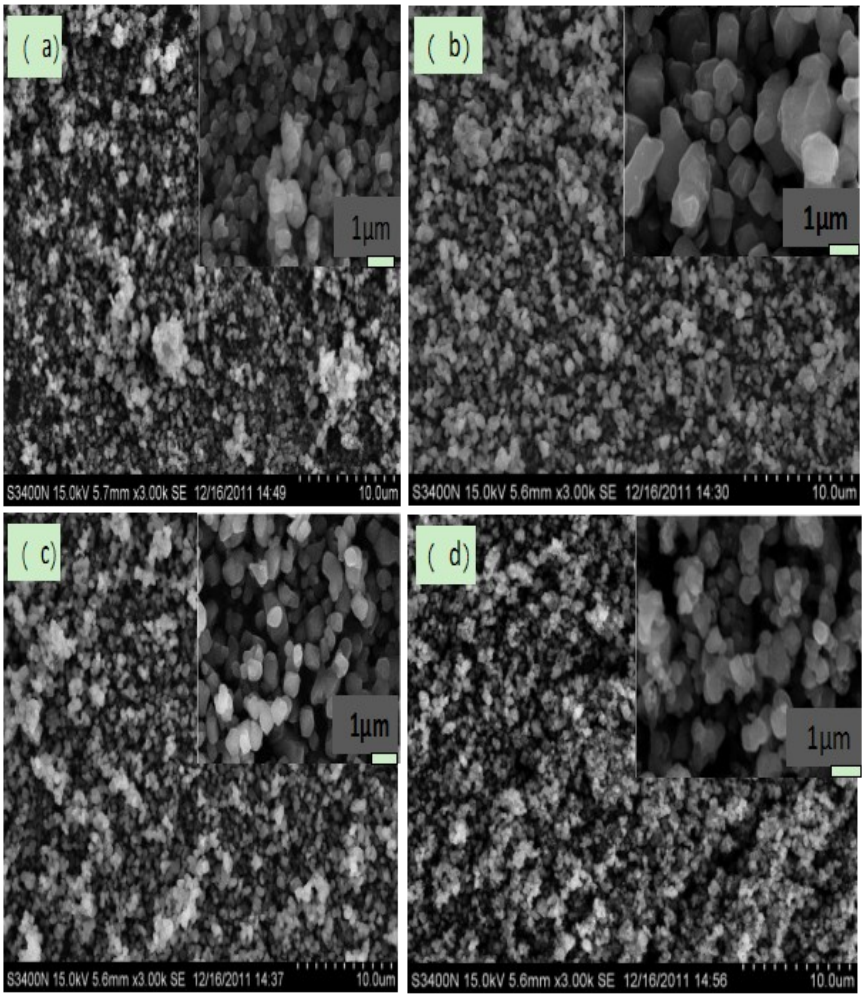

Figure 2. SEM images of (a) unimproved Sample A, (b) annealed Sample A, (c) unimproved sample B, and (d) annealed sample B.

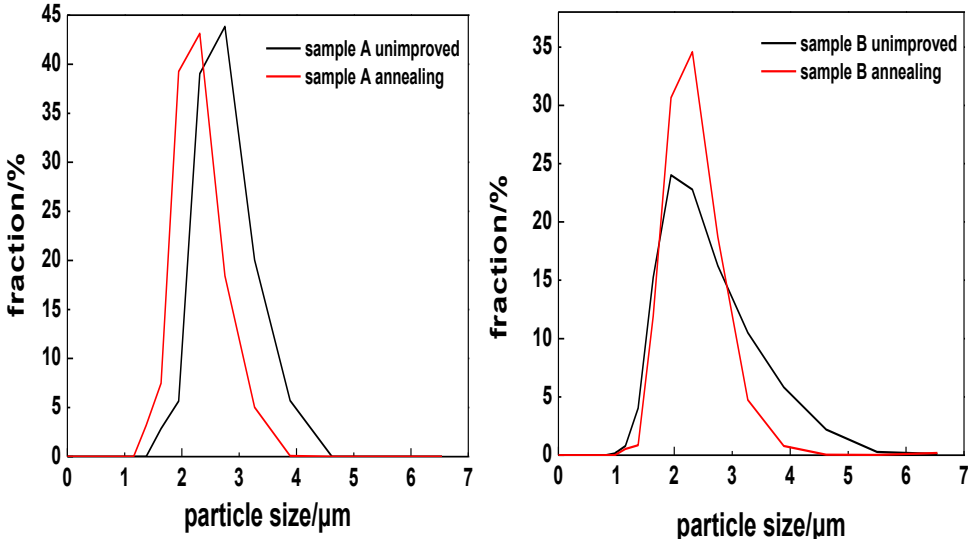

Figure 3. Particle size distribution of (a) unimproved Sample A, (b) annealed Sample A, (c) unimproved sample B, and (d) annealed sample B.

an average particle size of about 1 μm. Comparing the annealed and unimproved particles revealed that the latter had much larger micro-sized particles with a heavy degree of aggregation between neighboring particles. However, after annealing at 650 °C for 4 h, the particle distributions of samples A and B became uniform. Thus, annealing can result in high-surface-area LTO particles with a small degree of aggregation.

3.3. BET measurement and Particle size distribution (PSD)

The particle size distribution for the samples A and B with and without annealing is shown in Fig.3. It can be seen that the size is uniformly distributed for annealing samples. The average diameter of annealing Sample A (2.5μm) and Sample B (2.3μm) is smaller than unimproved Sample A (3.1μm) and Sample B(2.7μm). It may be due that particle is refined under annealing. The smaller particle is benefit for the improvement of rate capacity, and the uniformly distribute particle can enhance the cycle performance of battery.

The specific surface area of annealing Samples A and B was determined to be 3.4m^2/g and 5.7 m^2/g by the Brunauer-Emmett-Teller (BET) method, is higher than that of the improvement Samples A (3.2 m^2/g) and B (5.3 m^2/g). The higher specific surface area of active substance can increase its contact with electrolyte, further, improving the electrochemical performances of battery.

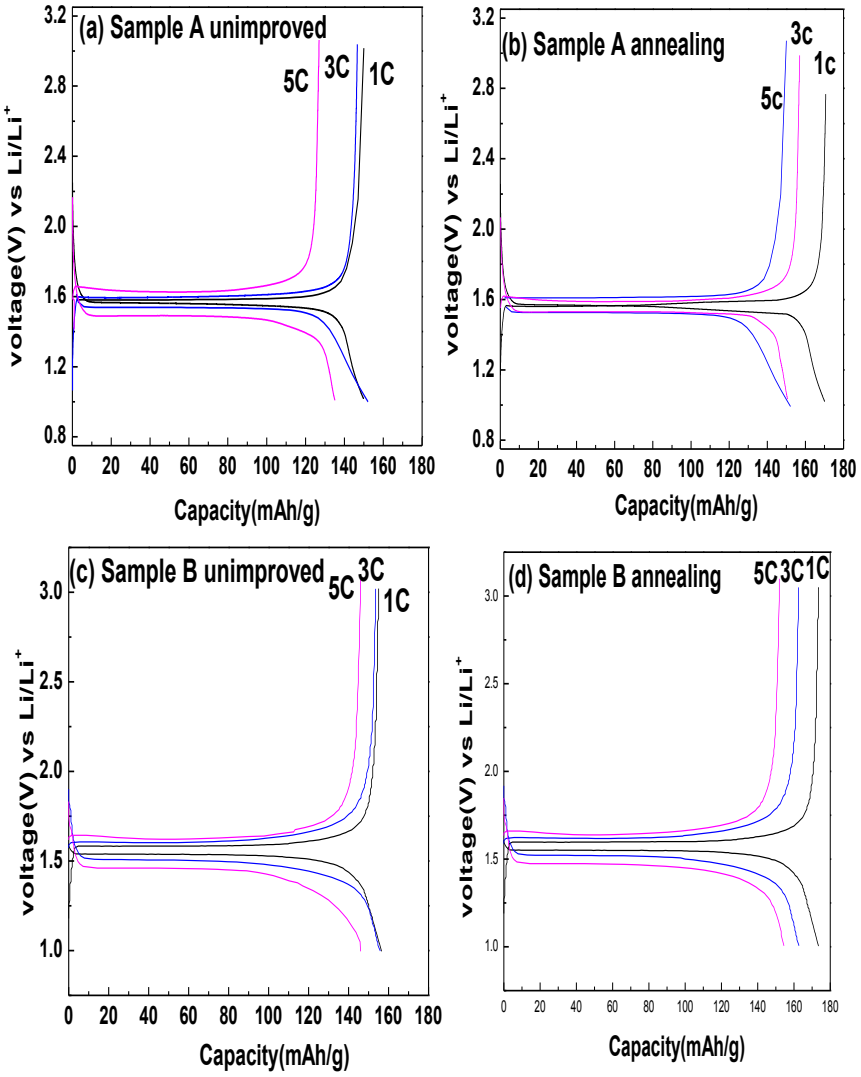

Figure 4. Charge–discharge curves at 1C rate of (a) unimproved sample A, (b) annealed sample A, (c) unimproved sample B, and (d) annealed sample B.

3.4. Galvanostatic charge-discharge measurement

Fig. 4 shows the electrochemical performances of samples A and B with and without annealing. The annealed LTO particles had a much higher specific capacity and better capacity retention than the unimproved LTO particles.

As shown in Figs. 2(a) and 2(b), after 650 °C insulation for 4 h under annealing, the first discharge capacity of sample A at the rates of 1C, 3C, and 5C were 170.7, 164.5, and 151.8 mAh·g^{-1}, respectively. Compared with the unimproved samples, the discharge capacities were almost improved. A charging and discharging platform was clearly observed at around 1.56 V.

Similarly, as shown in Figs. 2(c) and 2(d), the first discharge capacity of sample A at the rates of 1C, 3C, and 5C were 163.9, 147.9, and 141 mAh·g^{-1}, respectively. Compared with the unimproved samples, the discharge capacity also improved. Large-sized particles and inter-particle aggregation may be responsible for the low capacity and poor capacity retention of the unimproved sample.

Fig. 5 shows the cycling performance of annealed and unimproved LTO at the rates of 1C, 3C, and 5C. After 80 charge and discharge cycles, the discharge capacities of sample A were 161.5, 144.1, and 133.1 mAh·g^{-1}, and those for sample B were 163.9, 147.9, and 141 mAh·g^{-1}, respectively. The cyclic stability approach was used in the unimproved samples. The discharge capacities of the samples subjected to annealing at the rates of 1C, 3C, and 5C were still higher than those of the unimproved samples.

An overall comparison of the two samples revealed that the retention capacity rates for sample A were 94.6%, 87.6%, and 87.6%, and the retention capacity rates for sample B were 94.6%, 87.6%, and 87.6%. The charge–discharge property and cycling performance of sample B were much better than those of sample A. The main reason was that sample B contained carbon, which increased the electronic conductivity. The contact area increased the activity of the material and electrolyte, thereby improving Li ion transport.

4. CONCLUSIONS

The high rate capability of commercial LTO is improved by annealing. Commercial LTO particles are calcined at a 650 °C in 4 h. After annealing, the particle sizes decreased and particle distribution became more uniform. Ideal particle size distribution leads to good electrochemical properties. At the rates of 1C, 3C, and 5C, the discharge capacity of sample A reached 170.7, 164.5, and 151.8 mAh·g^{-1}, respectively, and that of sample B reached 173.6, 162.7, and 153.5 mAh·g^{-1}. Hence, the annealed samples significantly improved compared with the unimproved samples. After 80 charging and discharging cycles, the capacity retentions of sample A were 94.6%, 87.6%, 87.6%, respectively. The capacity retentions of sample A were 94.1%, 90.9%, and 91.8%, respectively. The cycle stability approach was used in the unimproved samples, and the discharge capacities of the annealed samples were still higher than those of the unimproved. The comparison of the electrochemical performances of samples A and B showed that the annealing process clearly affected the carbon-containing samples mainly because carbon itself has good conductivity. By contrast, carbon coatings inhibit the grain growth of LTO; smaller grain sizes shorten the diffusion path of Li^+ and promote reversible material capacities. Therefore, annealing is a very effective method for improving the performance of LTO. The method is easy to operate and suitable for the mass production of lithium-ion batteries.

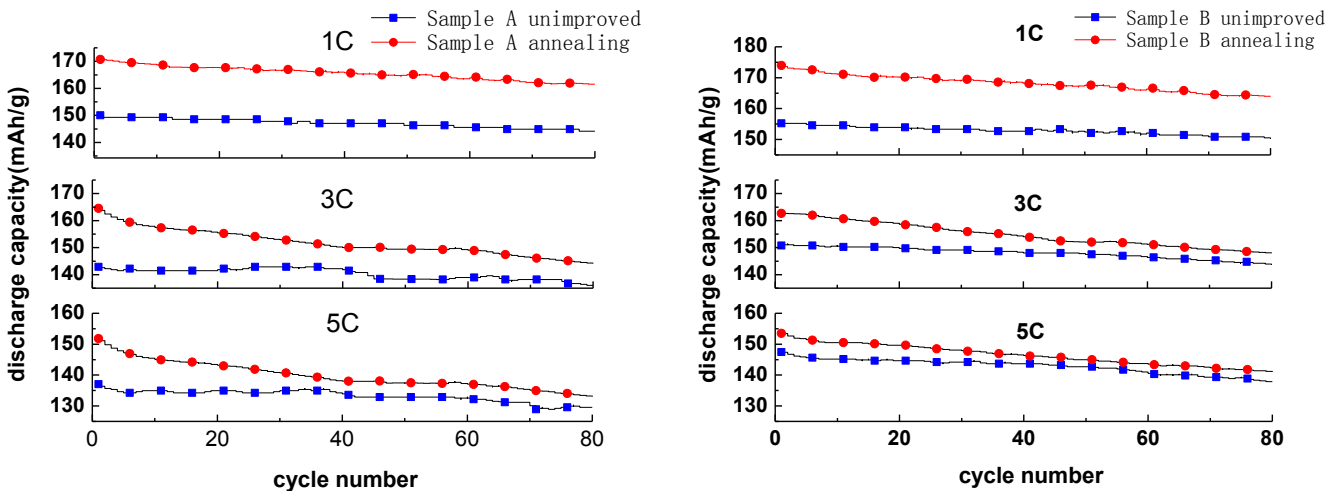

Figure 5. Cycling performances of (a) unimproved sample A, (b) annealed sample A, (c) unimproved sample B, and (d) annealed sample B.

5. ACKNOWLEDGEMENTS

This work was financially supported by Bid-invitation for Breakthroughs in Guangdong and Hong Kong key Areas (2010498E21), Guangdong Science and Technology Special (2009A080208001), and 2011 Key Technical Project of Strategic Emerging Industries(2011A010802001).

REFERENCES

[1] R.F. Nelson, J. Power Sources. 91. 2 (2000).
[2] C. Jiang, E. Hosono, H. Zhou. Nanotoday, 1, 28 (2006).
[3] Zhonghao Rao, Shuangfeng Wang. Renewable & Sustainable Energy Reviews, 15, 4554 (2011).
[4] A.D. Robertson, H. Tukamoto, J.T.S. Irvine, J. Electrochem. Soc. 146, 3958 (1999).
[5] T. Doi, Y. Iriyama, T. Abe, Z. Ogumi, Chem. Mater., 17, 1580 (2005).
[6] S.C. Lee, S.M. Lee, J.W. Lee, J.B. Lee, S.M. Lee, S.S. Han, H.C. Lee, H.J. Kim, J. Phys. Chem., C 113, 18420 (2009).
[7] K. Kataoka, Y. Takahashi, N. Kijima, H. Hayakawa, J. Akimoto, K. Ohshima, SolidState Ionics, 180, 631 (2009).
[8] K.C. Hsiao, S.C. Liao, J.M. Chen, Electrochim. Acta 53 (2008) 7242.
[9] Nakayama M., Ishida Y., Ikuta H. et al., Solid State Ionics, 117, 265 (1999).
[10]Z. Wen, Z. Gu, S. Huang, J. Yang, Z. Lin, O. Yamamoto, J. Power Sources, 146, 670 (2005).
[11]Y. Hao, Q. Lai, Z. Xu, X. Liu, X. Ji, Solid State Ionics, 176, 1201 (2005).
[12]M. Wagemaker, E.R.H. van Eck, A.P.M. Kentgens, F.M. Mulder, J. Phys. Chem., B113, 224 (2009).
[13]P. Reale, S. Panero, F. Ronci, V. Rossi Albertini, B. Scrosati, Chem. Mater., 15, 3437 (2003).
[14]Scrosati B., Panero S., Reale P. et al., J. Power Sources, 105, 161 (2002).
[15]G.J. Wang, J. Gao, L.J. Fu, N.H. Zhao, Y.P. Wu, T. Takamura, J. Power Sources, 173, 1109 (2007).
[16]X.L. Yao, S. Xie, H.Q. Nian, C.H. Chen, J. Alloys Compd., 465, 375 (2008).
[17]Y. Yu, J.L. Shui, C.H. Chen, Solid State Commun., 135, 485 (2005).
[18]G. Wang, J. Xu, M. Wen, R. Cai, R. Ran, Z. Shao, Solid State Ionics, 179, 946 (2008).
[19]E. Matsui, Y. Abe, M. Senna, A. Guerfi, K. Zaghib, J. Am. Ceram. Soc., 91, 1522 (2008).
[20]N.A. Alias, M.Z. Kufian, L.P. Teo, S.R.Majid, A.K. Arof, J. Alloys Compd., 486, 645 (2009).
[21]S.H. Ju, Y.C. Kang, J. Phys. Chem. Solids, 70, 40 (2009).
[22]D. Yoshikawa, Y. Kadoma, J.M. Kim, K. Ui, N. Kumagai, N. Kitamura, Y. Idemoto, Electrochim. Acta, 55, 1872 (2010).
[23]D.H. Kim, Y.S. Ahn, J. Kim, Electrochem. Commun., 7, 1340 (2005).
[24]L.C. Yang, Q.S. Gao, Y.H. Zhang, Y. Tang, Y.P. Wu, Electrochem. Commun., 10, 118 (2008).
[25]Elly Setiawati, Masahiko Hayashi, Masaya Takahashi, Takahisa Shodai, Keiichi Saito. J. Power Sources, 196, 10133 (2011).
[26]Seung-Ho Yu, Andrea Pucci, Tobias Herntrich, Marc-Georg Willinger, Seung-Hwan Baek, Yung-Eun Sungac and Nicola Pinna, J. Materials Chemistry, 21, 806 (2011).